ATMOSPHERE, IONOSPHERE, SAFETY

Part 1

Kaliningrad
2018

IMMANUEL KANT BALTIC FEDERAL UNIVERSITY
SEMENOV INSTITUTE OF CHEMICAL PHYSICS, RAS
PUSHKOV INSTITUTE OF TERRESTRIAL MAGNETISM, IONOSPHERE
AND RADIO WAVE PROPAGATION, RAS

ATMOSPHERE, IONOSPHERE, SAFETY

Proceedings
of VI International conference

Part 1

Kaliningrad
2018

UDK 550.51
BBK 552.44
A92

The conference AIS-2018 was supported by Russian Foundation for Basic Researches (Grant No. 18-03-20020); the VarSITI program and the program «5-100» for improving competitiveness at Immanuel Kant Baltic Federal University.

A92 **Atmosphere, ionosphere, safety** / edited by I. V. Karpov, O.P. Borchevkina. — Kaliningrad, 2018. — Pt. 1 — 360 p.
ISBN 978-5-9971-0490-0 (Pt. 1)
ISBN 978-5-9971-0491-7

Proceedings of International Conference "Atmosphere, ionosphere, safety" (AIS-2018) include materials reports on: (1) — response analysis of the atmosphere — ionosphere to natural and manmade processes, various causes related geophysical phenomena and evaluate possible consequences of their effects on the human system and process; (2) — to study the possibility of monitoring and finding ways to reduce risk. Scientists from different countries and regions of Russia participated in the conference. Attention was given to questions interconnected with modern nanotechnology and environmental protection. Knowledge of the factors influencing the atmosphere and ionosphere can use them to monitor natural disasters and to establish the appropriate methods on this basis.

Content of the reports is of interest for research and students specializing in physics and chemistry of the atmosphere and ionosphere.

UDK 550.51
BBK 552.44

ISBN 978-5-9971-0490-0 (Pt. 1)
ISBN 978-5-9971-0491-7

7. J.-W. Lin, Two-dimensional ionospheric total electron content map (TEC) seismo-ionospheric anomalies through image processing using principal component analysis, *Adv. Space Res.,* 2010, 45(11), pp. 1301—1310, doi:10.1016/j.asr.2010.01.029.
8. M. Akhoondzadeh, A MLP neural network as an investigator of TEC time series to detect seismo-ionospheric anomalies, *Adv. Space Res.,* 2013, 51(11), pp. 2048—2057, doi: 10.1016/j.asr.2013.01.012.
9. M. Akhoondzadeh, Genetic algorithm for TEC seismo-ionospheric anomalies detection around the time of the Solomon (Mw = 8.0) earthquake of 06 February 2013, *Adv. Space Res.,* 2013, 52(4), pp. 581—590, doi: 10.1016/j.asr.2013.04.012.
10. S. A. Pulinets and K. G. Tsybulya, Unique variations of the total electron content in the preparation period of Haitian earthquake (M7.9) on January 12, 2010, *Geomagn. Aeron.,* 2010, 50(5), pp. 686—689, doi: 10.1134/S0016793210050166.
11. H. Le, J. Y. Liu, and L. Liu, A statistical analysis of ionospheric anomalies before 736 M 6.0+ earthquakes during 2002—2010, *J. Geophys. Res.,* 2011, 116(A2), A02303. doi:10.1029/2010JA015781.
12. T. Xu, Zhi Chen, Chunbin Li et al. GPS total electron content and surface latent heat flux variations before the 11 March 2011 M9.0 Sendai earthquake, *Adv. Space Res.,* 2011, 48(8), pp. 1311—1317, doi:10.1016/j.asr.2011.06.024.
13. S. A. Pulinets, V. G. Bondur, M. N. Tsidilina, and M. V. Gaponova, Verification of the concept of seismoionospheric coupling under quiet heliogeomagnetic conditions, using the Wenchuan (China) earthquake of May 12, 2008, as an example, *Geomagn. Aeron.,* 2010, 50(2), pp. 231—242, doi:10.1134/S0016793210020118.
14. B. A. Carter, A. C. Kellerman, T. A. Kane et al., Ionospheric Precursors to Large Earthquakes: A Case Study of the 2011 Japanese Tohoku Earthquake, *J. Atm. Solar-Terr. Phys.,* 2013, 102, pp. 290—297, doi:10.1016/j.jastp.2013.06.006.
15. D. V. Davidenko, PhD thesis, Diagnostic of ionosphere disturbances ove seismic regions, Moscow, 2013. URL: http://ipg.geospace.ru/ref/20130716/auto_Davidenko.pdf (in Russian)
16. L. He, L. Wu, S. Pulinets et al., A nonlinear background removal method for seismo-ionospheric anomaly analysis under a complex solar activity scenario: A case study of the M9.0 Tohoku earthquake, *Adv. Space Res.,* 2012, 50, pp. 211—220, doi:10.1016/j.asr.2012.04.001

Nonlinear Interaction of Wave Processes in the Middle and Upper Atmosphere

Ksenia A. Didenko[1] and Alexander I. Pogoreltsev[1,2]

[1]Department of Atmospheric physics, St Petersburg University, St.Petersburg-Petrodvorets,198904, Russia
[2]Department of Meteorological Forecasting, Russian State Hydrometeorological Universty, St.Petersburg,195196, Russia

Introduction. In the stratosphere, there is anti-correlation between changes in the amplitudes of stationary planetary waves with zonal wave numbers 1 and 2 (SPW1 and SPW2). This negative correlation is mainly due to the nonlinear wave-wave interactions within the stratosphere. To interpret the observed behavior of

SPW amplitudes, it is useful to consider the nonlinear interactions of SPWs with the zonal mean flow and between the SPWs with different zonal wave numbers. Using this approach, the conservation of the perturbed potential enstrophy is investigated. When the amplitude of the SPW considered changes, the transfer of energy or enstrophy to another wave numbers is a necessary condition for the maintenance of the conservation requirements. In this case the terms responsible for the wave-wave interaction in the balance equation of the potential enstrophy (Ertel's potential vorticity squared) are calculated [1].

To obtain the balance equation of potential enstrophy, we use the linearized equation of conservation of the potential vorticity and multiply it by its eddy component and include the source and/or sinks term Q:

$$q' \times \quad D_t q' + v' \, \bar{q}_\varphi / a + w' \, \bar{q}_z = Q' \tag{1}$$

where

$$D_t \equiv \partial/\partial t + (\bar{u}/a \cos\varphi) \, \partial/\partial\lambda \tag{2}$$

$$Q = \frac{Rf}{H\rho} \frac{\partial}{\partial z} \frac{\rho D}{N^2} \tag{3}$$

(here R is the gas constant of dry air, f is Coriolis force, H is height scale, ρ is the background density, D is the rate of temperature change due to diabatic heating and N represents the buoyancy frequency.

The result is the general form of the eddy enstrophy balance:

$$\frac{\partial}{\partial t} \frac{\overline{q'^2}}{2} + \overline{\frac{q'u'}{a\cos\varphi} \frac{\partial q'}{\partial\lambda}} + \overline{\frac{q'v'}{a} \frac{\partial q'}{\partial\varphi}} + \frac{\overline{q'v'}}{a} \frac{\partial\bar{q}}{\partial\varphi} = \overline{q'Q'} \tag{4}$$

where q' is the perturbation of the quasi-geostrophic potential vorticity, u' and v' are perturbations of the zonal and meridional geostrophic winds, and Q' represents the perturbation of diabatic sources and sinks and terms describing the subscale contributions to the momentum equation. All other symbols have their conventional meaning: a is the Earth's radius, λ and φ are the longitude and latitude. The first term in left-hand side denotes the wave transience. The two next terms describe the wave-wave interactions. The last term in the left-hand side describes the eddy enstrophy changes due to wave-mean flow interaction. The term in the right-hand side gives the changes in eddy enstrophy due to the diabatic heating and subscale contributions to the momentum equation including momentum deposition by gravity and inertial-gravity waves [1].

Decomposing into series potential vorticity, zonal and meridional winds and diabatic heating for the zonal wavenumbers 1, 2, 3 and substituting to Equation (4) we can calculate the contribution of different terms to the eddy enstrophy balance for SPW1 and SPW2 (in a similar way with the expressions that was suggested by Smith (1983, Appendix [1])). The terms describing the interactions SPW1 and SPW2 may be written as follows:

$$+\frac{1}{4a\cos\varphi}[2U_2 Q_1^2 Q_1^{*2} + U_2^*(Q_1^{*2} - Q_1^2)] +$$

$$+\frac{1}{4a}\left[(V_2 Q_1 + V_2^* Q_1^*)\frac{\partial}{\partial\varphi} Q_1 + (V_2^* Q_1 - V_2 Q_1^*)\frac{\partial}{\partial\varphi} Q_1^*\right] \tag{5}$$

while Smith et al. (1984) suggested that this term can be rewritten in a different way using the quasi-geostrophic eddy continuity equation for SPW2 [2]:

$$+\frac{1}{8a\cos\varphi}\frac{\partial}{\partial\varphi}\{[V_2(Q_2^1 - Q_1^{*2}) + 2V_2^*(Q_1Q_1^*)]\cos\varphi\} \tag{6}$$

Comparison of the results obtained using expressions (5) and (6) shows that there are significant differences between them (at least in the middle latitudes of the winter stratosphere, where the nonlinear wave-wave interactions are strong). [3]

For a correct description of nonlinear interactions, it is necessary to refuse the quasi-geostrophic approximation. A quasi-geostrophic potential vortex which perturbation is used for calculating the perturbation of the potential enstrophy is not an approximation of the Ertel's potential vorticity. It is just its analogue (even the dimension is different). Taking into account the expression for the absolute vorticity $\omega_a = rotV + 2\Omega$, $\Omega = \{0, \Omega\cos\varphi, \Omega\sin\varphi\}$ and neglecting $2\Omega\cos\varphi$ in comparison with the vertical derivative of the zonal wind u_z, we obtain the expression for the Ertel's potential vorticity $P = \omega_a \cdot \nabla\theta / \rho_0$, which is usually used in atmospheric dynamics, particularly in "primitive" equations in a spherical coordinate system [4]. To compare the results obtained with the quasi-geostrophic approximation and without it, we should use $P' \cdot \frac{\rho_0}{\theta_z}$ instead of q' in the eddy enstrophy balance equation (4).

In order to show the behavior of different terms in the balance of potential enstrophy using q' or $P' \cdot \frac{\rho_0}{\theta_z}$, it was decided to consider an example of simulation with the middle and upper atmosphere model (MUAM) when a strong sudden stratospheric warming (SSW) was observed (simulated). Wave activity usually intensifies during this phenomenon. Fig. 1 demonstrates the results of simulation with the MUAM (a set of the ensemble runs for El-Nino conditions have been performed and one of the ensemble runs was selected). One can see a strong increase in the amplitude of the SPW1 on the 10th of January, which was accompanied by reversal of the zonal mean flow in the stratosphere. As a consequence, the sudden stratospheric warming was observed several days later.

Using the results of simulation, the terms of Equation (4) were calculated and visualized. The values have been averaged over the middle latitude region from 57.5 to 72.5°N, using cosine of latitude weighting. The results in Fig. 2a and 3a shows that the time changes of eddy potential enstrophy for SPW1 and SPW2 are almost independent on the type of the potential vorticity is used. The run of the curve showing the interaction between waves with different wave numbers looks similar (weather we use q' or $P' \cdot \frac{\rho_0}{\theta_z}$), but the intensity is noticable different. The most interesting situation is formed when considering the interaction of the SPW1 or SPW2 with the mean flow. In the panel (d) of Fig. 2 and 3 one can see, that the values of interaction terms for quasi-geostrophic potential vorticity and Ertel's potential vorticity are out of phase.

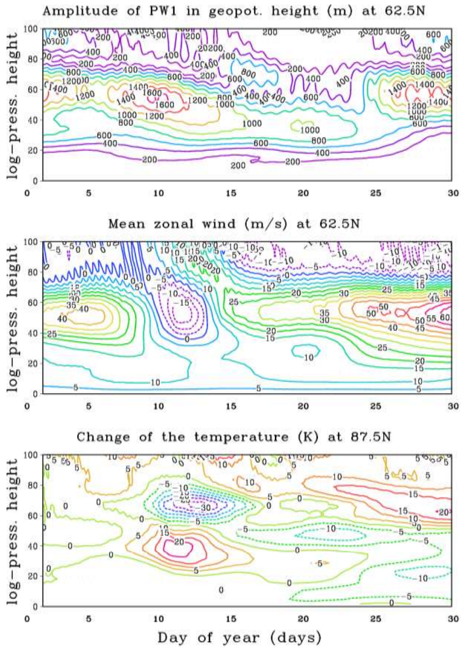

FIGURE 1. The time-altitude cross-sections of the amplitude of zonal harmonic with zonal wave number m = 1 in the geopotential height and the mean zonal wind at latitude 62.5N (upper and middle panels) for January; the changes of the zonal mean temperature during this month at 87.5N are shown in the lower panel. MUAM data.

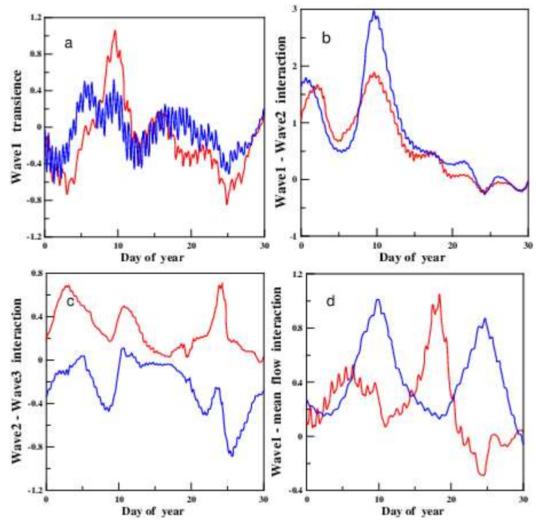

FIGURE 2. Terms contributing to the eddy enstrophy balance (using quasi-geostrophic potential vorticity — red lines (grey lines in black-and-white), Ertel's potential vorticity — blue ones (black lines in black-and-white)) for SPW1 at 30 km for January: (a) transience, (b) wave1-wave2 and (c) wave2-wave3 interaction and (d) wave–mean flow interaction. Units are 10^{-15} s^{-3}.

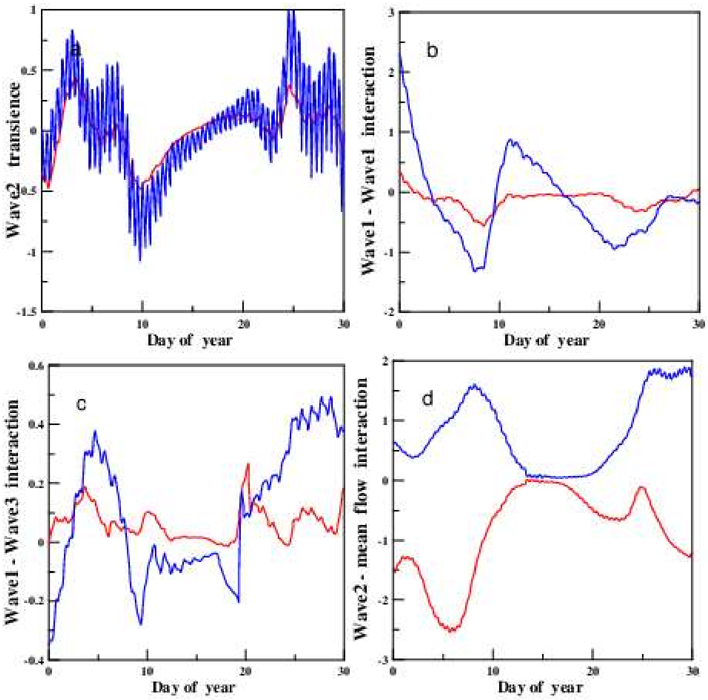

FIGURE 3. Terms contributing to the eddy enstrophy balance (using quasi-geostrophic potential vorticity — red lines (grey lines in black-and-white), Ertel's potential vorticity — blue ones (black lines in black-and-white)) for SPW2 at 30 km for January: (a) transience, (b) wave1-wave1 and (c) wave1-wave3 interaction and (d) wave-mean flow interaction. Units are 10^{-15} s^{-3}.

Conclusion. The results of calculation the terms in the eddy potential enstrophy balance equation demonstrate substantial differences between the quasi-geosptrophic approximation and when we use the Ertel's potential vorticity expression. It is important to consider in more details the interaction of SPW1 and SPW2 with the mean flow separately. Moreover, terms containing a vertical velocity were not considered in this research. These terms can provide a contribution to the balance during the SSW events and/or in the case of nonlinear interaction between higher-frequency planetary waves (for instance, the atmospheric tides). This problem will be the subject of a further research.

1. A. K. Smith, *J. Atmos. Sci.*, 1983, vol 40, pp. 2484—2493.
2. A. K. Smith, *J. Atmos. Sci.*, 1984, vol 41, No.3, p. 365.
3. A. I. Pogoreltsev, E. N. Savenkova, O. G. Aniskina, T. S. Ermakova, W. Chen, K. Wei, *J. Atmos. Solar-Terr. Phys.,* 2015, pp. 191—194.
4. D. G. Andrews, J. R. Holton, B. L. Conway, *UK: ACADEMIC PRESS INC. (LONDON) LTD*, 1987, pp. 120—122.